A STATE BOUNDING OBSERVER BASED ON ZONOTOPES

C. Combastel

ECS-ENSEA, 6 avenue du ponceau, 95014 Cergy-Pontoise, France
tel: +33 (0)1 30 73 62 64
fax: +33 (0)1 30 73 66 27
e-mail: combastel@ensea.fr

Keywords: Observer, state bounding, zonotopes, bounded error, set-membership estimation.

Abstract

The proposed observer computes an outer approximation of the set of states which are consistent with a given uncertain state space model and some measurements. The uncertainties are modeled by unknown but bounded inputs. A representation of domains by zonotopes (particular polytopes) is used to reduce the computation of state bounds to rather simple matrix operations and to control the wrapping effect.

1 Introduction

Given a model and some measurements, an observer aims at providing information on the state of the system. In practice, the exact modeling of a real system is almost impossible and measurements are often corrupted by noise. Due to such uncertainties, the precision of the available knowledge on the system (model and measurement) is necessarily bounded. Therefore, uncertainties have to be taken into account for the state estimation to remain consistent with the available knowledge. The approaches used to design observers can be classified according to how they deal with uncertainties [4]. Some of them do not take explicitly the uncertainties into account, such as Luenberger observers. A statistical modeling of uncertainties can also be used: state estimators based on Kalman filters [9] belong to this kind of approaches. Assumptions about the distribution of the random variables modeling the (state and measurement) perturbations have to be done, but may be difficult to validate. The last group of methods relies on the description of uncertainties by known compact sets (in $\Re^n$: bounded and closed sets). No assumption about the statistical properties is then required. The result of state estimation is a domain (compact set) in the state space representing an outer approximation of all the states that are consistent both with the uncertain model and the uncertain measurements. This makes these approaches attractive for fault diagnosis [2], [8] or localization [1] applications, for instance. Several representations of domains can be used when designing state bounding observers: ellipsoids, orthotopes (boxes), parallelotopes or polytopes with limited complexity (i.e. with a limited number of faces and vertices). Among them, ellipsoids are certainly the most widely used [3]. The present paper focuses on the representation of domains by zonotopes [7], which correspond to a particular class of polytopes. More precisely, a zonotope is the image of a (unit) hypercube by a linear application. An appropriate representation of domains results from a compromise between the exactness (outer approximations are not too pessimistic) and the required computation load. For instance, polytopes may be used to represent exactly the domains in a linear context; but if the number of faces and vertices increases at each integration step, the computation load becomes quickly prohibitive. That is why the state bounding observer presented in this paper implements a step performing a reduction of the zonotope complexity, in addition to a prediction step and a correction step. The later two steps are similar to those implemented in Kalman filters: prediction makes use of the uncertain model whereas correction makes use of the uncertain measurements to update the state estimation. The use of zonotopes to implement the prediction step and the reduction step has been largely inspired by the work of W. Kühn [5], [6], [7]. This work aims at computing mathematical rigorous error bounds for the numerical approximation of discrete dynamical systems. Zonotopes are shown to be a suitable representation in order to control the wrapping effect[1]. The main originality of the present work is to add a correction step in order to design a state bounding observer.

The paper is organized as follows: the first section deals with the definition of the class of uncertain dynamical systems that is used to design the proposed state bounding observer. The second section defines the zonotopes and gives some of their properties. The principle of bounded error state estimation is recalled in the third section. Then, the prediction step, the reduction step and the correction step are successively detailed. Finally, the fourth section shows simulation results.

1 Problem formulation

Some notations are first introduced. The real interval [-1;1] will be denoted by an empty square: $\square = [-1;1]$. Moreover, the name of a variable v in brackets, $[v]$, will denote a domain of possible values for v: $v \in [v]$.

[1] Wrapping effect: (possibly unstable) growth of domains due to the cumulative uncertainty resulting from the outer approximations at each step when integrating a dynamical system.

The class of systems under study is that of discrete linear time varying systems with additive and bounded uncertainties:

$$\begin{aligned} x_{k+1} &= A_k.x_k + B_k.u_k + E_k.v_k \\ y_k &= C_k.x_k + D_k.u_k + F_k.w_k \end{aligned} \quad \text{where} \quad \begin{aligned} v_k &\in \square^n \\ w_k &\in \square^m \end{aligned} \qquad (1)$$

$$x_k \in \Re^n,\ u_k \in \Re^q,\ y_k \in \Re^m$$

x_k, u_k, y_k are column vectors respectively representing the state, the input and the measurement of the system. As no model can exactly represent the system state and measurement given only the known input, the validity of the model (1) is restored by modeling uncertainties with two additive unknown inputs: v_k and w_k. v_k stands for the state perturbation whereas w_k stands for the measurement perturbation (offset, noise, etc…). Instead of assuming statistical properties for v_k and w_k as in Kalman filtering, they are only assumed to be bounded: v_k (resp. w_k) belongs to a n (resp. p) dimensional hypercube (1). A_k, B_k, C_k, D_k, E_k, F_k are known real matrices of appropriate dimensions. F_k is assumed to be invertible. Moreover, the initial state of the system is assumed to belong to a known domain (that may be chosen large to represent a lack of available information on the system initial state):

$$x_0 \in [\hat{x}_0] \qquad (2)$$

Given the model (1), y_k and u_k, the problem of designing a state bounding observer consists in computing an outer approximation $[\hat{x}_k]$ of the domain of possible values for the unknown state x_k. For the precision of the state estimation to be as good as possible, $[\hat{x}_k]$ should be of minimal size while still guaranteeing that the relation $x_k \in [\hat{x}_k]$ holds. An optimal minimization of the domain size is often a difficult task. However, the choice of an appropriate domain representation can help to compute not too pessimistic outer approximations. This will be the subject of the next section.

Remark: Most of the time, x_k is bounded due to physical limits. When the system is observable (or, at least, detectable), the sensors often provide more precise information on x_k than these physical bounds. However, when the system is not observable and not detectable, the physical bounds of the state represent the only available information to perform a correction step. Modeling such bounds can be done by introducing artificial measurements in the model (1) as:

$$\begin{bmatrix} y_k \\ 0 \end{bmatrix} = \begin{bmatrix} C_k \\ I \end{bmatrix}.x_k + \begin{bmatrix} D_k \\ 0 \end{bmatrix}.u_k + \begin{bmatrix} F_k & 0 \\ 0 & L \end{bmatrix}.w_k, \quad w_k \in \square^m \qquad (3)$$

For example, if the matrix L is diagonal in the modified measurement equation (3), each diagonal element has the meaning of a physical bound for the corresponding state in x_k.

2 Zonotopes: definition and properties

Zonotopes are a special class of convex polytopes. More precisely, a p-zonotope in $\Re^n$ is the Minkowski sum of p straight line segments in $\Re^n$. It can be also defined as the linear image of a p-dimensional hypercube in $\Re^n$. Some notations and examples will be given to illustrate these definitions and to state some of the zonotope properties. To begin with, the Minkowski sum of two sets, $[x]$ and $[y]$, is the set defined as:

$$[x]+[y] = \{x+y \,/\, x \in [x], y \in [y]\} \qquad (4)$$

A straight line segment in $\Re^n$, denoted $[S_i]$, can be defined by two column vectors: $c_i \in \Re^n$ stands for the segment center, and $r_i \in \Re^n$ defines both the direction and the radius of $[S_i]$:

$$[S_i] = c_i + r_i.\square \qquad (5)$$

Following the first definition, a p-zonotope, $[Z]$, is the Minkowski sum of p straight line segments, $[S_i]$, i=1…p:

$$[Z] = [S_1] + \cdots + [S_p] \qquad (6)$$

Substituting (5) for $[S_i]$, i=1…p, in (6), a second expression of $[Z]$ can be deduced:

$$[Z] = c + R.\square^p \qquad (7)$$

$$c = c_1 + \cdots + c_p, \quad R = [r_1 \cdots r_p] \qquad (8)$$

Except for the translation corresponding to the center c, (7) shows that the p-zonotope $[Z]$ can be defined as the linear image (by $R \in \Re^{n\times p}$) of the p-dimensional hypercube $\square^p$ ($\square^p$ will be called the abstract domain related to $[Z]$). The unary operator ◆ over the real matrices is used to denote such an image. (7) can be thus rewritten as $[Z] = c + \blacklozenge R$, where:

$$\blacklozenge R = R.\square^p, \quad R \in \Re^{n\times p} \qquad (9)$$

If R_1 and R_2 are identical up to a permutation of their column vectors, then $\blacklozenge R_1 = \blacklozenge R_2$. Figure 1 illustrates the previous definitions by showing the step by step construction of a zonotope generated by three straight line segments.

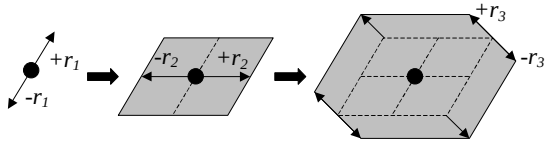

Figure 1: Construction of a 3-zonotope $[Z]$ in $\Re^2$

The zonotope definitions can be particularized in many ways and some links exist with other domain representations [5]: the unit cube is $\blacklozenge I$ where I is the identity matrix. If the $n\times n$ matrix R is (*i*) invertible, (*ii*) unitary: $R^T.R=I$, or (*iii*) diagonal, then $\blacklozenge R$ is (*i*) a parallelotope, (*ii*) a cube or (*iii*) an interval vector (i.e. a box aligned along the reference frame axes).

Following the previous definitions, some properties of centered zonotopes will be stated. Firstly, the (Minkowski) sum of two centered zonotopes in $\Re^n$ can be computed by a matrix concatenation:

$$\blacklozenge R_1 + \blacklozenge R_2 = \blacklozenge [R_1\ R_2] \qquad (10)$$

Secondly, the image of a centered zonotope by a linear application L can be computed by a standard matrix product:

$$L.(\blacklozenge R) = \blacklozenge(L.R) \tag{11}$$

Thirdly (and finally), the smallest centered interval vector containing $\blacklozenge R$ is called the interval hull of $\blacklozenge R$ and denoted $\blacksquare R$. It can be computed as follows ($R \in \Re^{n \times p}$):

$$\blacksquare R = \blacklozenge rs(R), \qquad rs(R)_{ii} = \sum_{j=1}^{p} \left| R_{ij} \right| \tag{12}$$

where *rs* stands for "row sum" and $rs(R)$ is a diagonal matrix defined as in (12). The interval hull (Figure 2) is interesting to compute easily an outer approximation of reduced complexity for a given zonotope. Apart from the intersection, it can be noticed that several basic operations involving zonotopes reduce to simple (and fast) matrix computations.

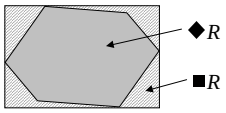

Figure 2: interval hull of a zonotope

3 Bounded error state estimation

The purpose of a state bounding observer is to find, in the state space, a minimal (if possible) outer approximation of the domain that is consistent both with the measurements and a given model of the system. In order to detail the algorithm steps, some notations are first introduced:

$[\hat{x}_{k/k'}]$ denotes the domain of possible states at time k resulting from the state space model of the system (1) and the measurements until time k' (time k' included). When k=k', the notation is simplified as: $[\hat{x}_k] = [\hat{x}_{k/k}]$.

$[\hat{x}_{k/y_k}]$ denotes the domain of possible states at time k resulting from the measurements at time k, y_k, and from the measurement equation in the system model (1).

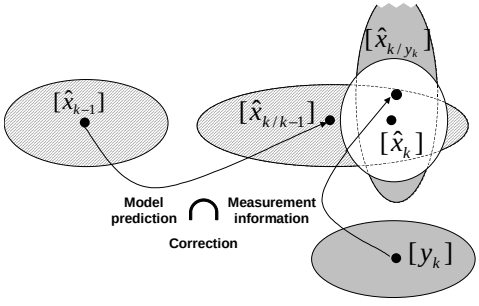

Figure 3: Principle of bounded error state estimation

$[\hat{x}_0]$ is used to initialize the algorithm (2). Assuming $[\hat{x}_{k-1}]$ is known, the state equation in (1) is used to compute $[\hat{x}_{k/k-1}]$. The prediction step is followed by a reduction step designed so as to control the zonotope complexity which would be else greater at each step. Finally, the correction step consists in computing an outer approximation of the intersection between $[\hat{x}_{k/k-1}]$ and $[\hat{x}_{k/y_k}]$ (Figure 3). The main loop of the state bounding algorithm is given in Figure 4. The main three steps it is composed of will be detailed in the following three subsections.

Initialization ($[\hat{x}_{1/0}]$ is computed from $[\hat{x}_0]$)
For k=1 to k_{max}
  System at time k: A_k, B_k, C_k, D_k, E_k, F_k, u_k, y_k
  $[\hat{x}_k] \leftarrow$ Correction($[\hat{x}_{k/k-1}]$, y_k, u_k)
  $[\hat{x}_{k+1/k}] \leftarrow$ Prediction($[\hat{x}_k]$)
  $[\hat{x}_{k+1/k}] \leftarrow$ Reduction($[\hat{x}_{k+1/k}]$)
End

Figure 4: Main loop of the state bounding algorithm

3.1 Prediction step

The prediction step aims at computing $[\hat{x}_{k+1/k}]$ from $[\hat{x}_k]$ and the state equation in the model (1). $[\hat{x}_k]$ is assumed to be a zonotope such that $x_k \in [\hat{x}_k]$. This membership relation holds at k=0 and the recurrence in Figure 4 will be shown to be designed so that the relation also holds at time k. To that purpose, $[\hat{x}_{k+1/k}]$ should be so that $x_{k+1} \in [\hat{x}_{k+1/k}]$. Let c_k and R_k respectively denote the center and the matrix generating the zonotope $[\hat{x}_k]$:

$$[\hat{x}_k] = c_k + \blacklozenge R_k \tag{13}$$

According to (1), $x_{k+1} = A_k.x_k + B_k.u_k + E_k.v_k$, on the one hand, according to the fact that $x_k \in [\hat{x}_k]$ and that $v_k \in \square^n$, on the other hand, it follows that $x_{k+1} \in [\hat{x}_{k+1/k}]$ where:

$$[\hat{x}_{k+1/k}] = A_k.[\hat{x}_k] + B_k.u_k + E_k.\square^n \tag{14}$$

Substituting (13) for $[\hat{x}_k]$ in (14), denoting respectively $c_{k+1/k}$ and $R_{k+1/k}$ the center and the matrix generating the zonotope $[\hat{x}_{k+1/k}]$, and applying (9), (10) and (11), it comes:

$$[\hat{x}_{k+1/k}] = c_{k+1/k} + \blacklozenge R_{k+1/k} \tag{15}$$

$$c_{k+1/k} = A_k.c_k + B_k.u_k \tag{16}$$

$$R_{k+1/k} = [A_k R_k \quad E_k] \tag{17}$$

The representation of domains by zonotopes reduces the prediction step to very simple matrix computations ((16) and (17)). Moreover, the prediction in itself is not subjected to any approximation. However, expanding the recurrence $R_{k+1} = [A_k R_k \quad E_k]$ (see note [2]) shows the need for a

[2] Identifying $R_{k+1/k}$ and R_{k+1} (by comparison with (17)) does not lead to a loss of generality as the only prediction step is studied here (i.e. the correction step and the reduction step can be momentarily viewed as identity operators).

reduction step: as R_0, A_k and E_k are $n\times n$ matrices, R_k is an $n\times n(k+1)$ matrix. Consequently, the number of segments generating the zonotope $[\hat{x}_{k+1/k}]$ is increased by n at each step if the prediction is considered alone. In order to control the domain complexity, a reduction step is thus implemented.

3.2 The reduction step

Let *Red* denote a reduction operator. *Red* is defined so as to map centered zonotopes into centered zonotopes and to map sets into supersets [7], [5]:

$$[Z] \subseteq Red([Z]) \tag{18}$$

As above mentioned, choosing the identity operator I_d for *Red* provides an exact solution but leads to a linear in k increase of the zonotope complexity. The interval hull (12) is another example of reduction operator. However, the outer approximations are then very pessimistic and the wrapping effect is most of the time prohibitive. Consequently, a compromise between exactness ($Red=I_d$) and reduced domain complexity ($Red=\blacksquare$) has to be found. To that purpose, an heuristic will be introduced. It is based on the fact that each segment generating a zonotope correspond to some edges of the final domain (Figure 1). An heuristic to reduce the complexity of a centered zonotope, $\blacklozenge R$, consists in finding an outer zonotope, $Red(\blacklozenge R)$, generated by less segments than $\blacklozenge R$, the edges of $\blacklozenge R$ with lower length having priority to be involved in the reduction. Following the proposed heuristic, the reduction algorithm is formalized. A parameter d defining the maximal zonotope complexity is chosen. d can be defined as the maximal number of $n\times n$ bloc matrices involved in $R_{k+1/k}$ (17). With no loss of generality, the centered zonotope to be reduced, $\blacklozenge R=\blacklozenge R_{k+1/k}$, is assumed to be generated by $p=n.d$ segments ($R_{k+1/k}$ can be completed with null column vectors to build R if $p<n.d$, $R=R_{k+1/k}$ otherwise):

$$\blacklozenge R = \blacklozenge[r_1 \ \cdots \ r_i \cdots \ r_p], \quad p=n.d \tag{19}$$

The column vectors of R are sorted on decreasing Euclidian norm. σ stands for the related index permutation. As a column permutation does not modify the zonotope, (20) holds:

$$\blacklozenge R = \blacklozenge[r_{\sigma(1)} \ \cdots \ r_{\sigma(i)} \cdots \ r_{\sigma(p)}], \quad \left\|r_{\sigma(i)}\right\| \geq \left\|r_{\sigma(i+1)}\right\| \tag{20}$$

$$\blacklozenge R = \blacklozenge[Q_1 \cdots \ Q_{d-2} \ \ Q_{d-1} \ \ Q_d] \tag{21}$$

The resulting matrix belongs to $\Re^{n\times nd}$. It can be thus written as the concatenation of d bloc matrices Q_j of size $n\times n$ (21). Then, the proposed reduction consists in replacing the zonotope generated by $[Q_{d-1}\ Q_d]$ by its interval hull:

$$\blacklozenge R \subseteq \blacklozenge[Q_1 \cdots Q_{d-2} \ N], \quad N = rs([Q_{d-1} \ Q_d]) \in \Re^{n\times n} \tag{22}$$

Such a reduction only operates on the generator segments (i.e. edges) of lower size, that is to say, those in Q_{d-1} and Q_d. The reduction operator in (22) can be also expressed as:

$$Red(\blacklozenge R) = \blacklozenge[Q_1 \cdots \ Q_{d-2}] + \blacksquare[Q_{d-1} \ Q_d] \tag{23}$$

The proposed reduction scheme makes it possible to set the zonotope complexity by choosing d. In other words, d allows to adjust the compromise between exactness (d is big) and reduced domain complexity (d is small). Other reduction strategies exist such as cascade reduction [5] or flush when full strategies [6]. The reduction proposed in this paper is easy to generalize when E_k is not a square matrix (1).

3.3 The correction step

The correction step aims at taking into account the information provided by the measurements at time k. Ideally, it would consist in computing the exact intersection between $[\hat{x}_{k/k-1}]$ and $[\hat{x}_{k/y_k}]$ (Figure 3). As rapidly computing the exact intersection of two zonotopes is not a trivial task, a zonotope only including the searched intersection will be computed in practice. One of the specifications was to reduce the correction step to standard and rather simple vector or matrix operations. In particular, solutions involving an enumeration of vertices or facets have not been considered for the overall algorithm to remain efficient from a real-time point of view. In the following, the correction problem will be first rewritten into a standard form. Then, the proposed correction step will be described. $[\hat{x}_{k/k-1}]$ is such that $x_k \in [\hat{x}_{k/k-1}]$. It can be decomposed into its center and a centered zonotope as:

$$[\hat{x}_{k/k-1}] = c_{k/k-1} + \blacklozenge R_{k/k-1} = c_{k/k-1} + R_{k/k-1}.\square^p \tag{24}$$

The measurement equation in the model (1) is:

$$y_k = C_k.x_k + D_k.u_k + F_k.w_k \tag{25}$$

Moreover, a prediction of the measurement at time k can be computed from the center of $[\hat{x}_{k/k-1}]$:

$$y_{k/k-1} = C_k.c_{k/k-1} + D_k.u_k \tag{26}$$

The difference between y_k and $y_{k/k-1}$ reflects the extra information provided by the measurement at time k compared to what can be deduced from the model. This difference is analogous to the innovation in the framework of Kalman filtering. From (25) and (26), it comes:

$$F_k^{-1}.(y_k - y_{k/k-1}) = F_k^{-1}.C_k.(x_k - c_{k/k-1}) + w_k \tag{27}$$

Let introduce the following notations to reformulate the correction problem at time k:

$$\delta = F_k^{-1}.(y_k - y_{k/k-1}), \quad M = F_k^{-1}.C_k$$
$$R = R_{k/k-1}, \quad w = w_k \tag{28}$$

δ, M and R can be computed at time k as they only depend on known variables. δ can be viewed as an innovation term that is normalized by the measurement uncertainties. Moreover, as $x_k \in [\hat{x}_{k/k-1}]$ and according to (24), there exist $s \in \square^p$ such that $x_k - c_{k/k-1} = R.s$. The correction problem can be thus expressed in the abstract space of $[\hat{x}_{k/k-1}]$ as finding an outer approximation $[s]$ of the intersection between $\square^p$ and the

domain of possible values for s resulting from the measurement equation (27). According to the notations introduced in (28), one way to formalize the correction problem at time k is the following: the correction problem at time k consists in finding an outer approximation $[s]$ of the s domain resulting from the three statements in (29):

$$s \in \square^p, \quad w \in \square^m, \quad \delta - w = MR.s \tag{29}$$

$[\hat{x}_k]$ is then computed from $[s]$ as:

$$[\hat{x}_k] = c_{k/k-1} + R.[s] \tag{30}$$

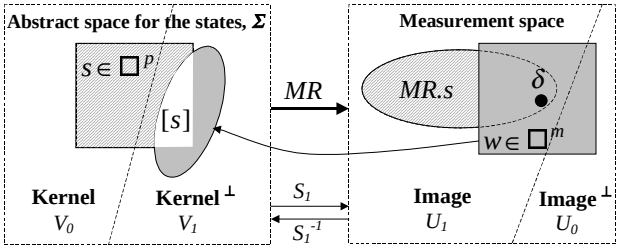

Figure 5: Illustration of the correction step

Before computing the intersection, the base of the abstract space, Σ, is changed in order to decompose it into two subspaces: the first subspace, generated by V_0, is the kernel of MR. It represents the subspace of Σ that is not influenced by δ (i.e. by the measurement at time k). The second subspace, generated by V_1, is the supplement to the kernel of MR. The inverse image of the measurement domain (centered on δ) defines a domain in this second subspace, where the intersection will take place (Figure 5). V_0 and V_1 are computed from a singular value decomposition of MR as:

$$MR = U.S.V^T = \begin{bmatrix} U_1 & U_0 \end{bmatrix} \begin{bmatrix} S_1 & 0 \\ 0 & 0 \end{bmatrix} \begin{bmatrix} V_1^T \\ V_0^T \end{bmatrix} \tag{31}$$

$U=[U_1\ U_0]$ and $V=[V_1\ V_0]$ are unitary matrices ($U^TU=I$, $V^TV=I$) and S_1 is a diagonal matrix where $diag(S_1)$ are the (nonzero) singular values of MR. Let σ_1 and σ_0 denote the coordinates of s in the new base. It comes:

$$s = V_1.\sigma_1 + V_0.\sigma_0 \quad \text{and} \quad \begin{bmatrix} \sigma_1 \\ \sigma_0 \end{bmatrix} = \begin{bmatrix} V_1^T \\ V_0^T \end{bmatrix} .s \tag{32}$$

According to (31) and (32), the last two statements in (29) are verified if (33) holds:

$$\sigma_1 \in [Z_1] = S_1^{-1} U_1^T \delta - \blacklozenge S_1^{-1} U_1^T \tag{33}$$

According to (32), the projection in the subspace generated by V_1 (resp. V_0) of the first statement in (29), $s \in \square^p$, can be expressed as:

$$\sigma_1 \in \blacklozenge V_1^T \quad (\text{resp. } \sigma_0 \in \blacklozenge V_0^T) \tag{34}$$

As a consequence of (33) and (34), the three statements in (29) hold when (35) holds:

$$\sigma_1 \in [Z_1] \cap \blacklozenge V_1^T \quad \text{and} \quad \sigma_0 \in \blacklozenge V_0^T \tag{35}$$

An intersection of two zonotopes is involved in (35). An outer approximation of this intersection by a box, $[B^{inter}]$, can be obtained by intersecting the interval hulls of the two zonotopes, which is an easy task (intersection of two boxes):

$$\sigma_1 \in [B^{inter}] = (S_1^{-1} U_1^T \delta - \blacksquare S_1^{-1} U_1^T) \cap (\blacksquare V_1^T) \tag{36}$$

(35) shows that the pessimism induced by such an approximation is limited to the subspace influenced by the measurements at time k (V_1). Pessimism does not affect the supplementary subspace (V_0), where only the model prediction provides information. This justifies the proposed decomposition of the abstract space Σ (Figure 5, (31) and (32)). $[B^{inter}]$ can be decomposed into its center, c^{inter} and a (diagonal) matrix R^{inter} as:

$$\sigma_1 \in [B^{inter}] = c^{inter} + \blacklozenge R^{inter} \tag{37}$$

As $s = V_1.\sigma_1 + V_0.\sigma_0$ (32), on the one hand, as $\sigma_1 \in [B^{inter}]$ (37) and $\sigma_0 \in \blacklozenge V_0^T$ (35), on the other hand, an outer approximation of the searched domain is computed as:

$$[s] = (V_1.c^{inter}) + \blacklozenge [V_1.R^{inter} \quad V_0.V_0^T] \tag{38}$$

Given $[s]$ (38), the correction step finally returns $[\hat{x}_k]$ from (30). Through the intersection step, the center of $[\hat{x}_k]$ does not only depend on the innovation (i.e. on y_k, u_k, $c_{k/k-1}$) but also on the dynamic evolution of the computed domains.

4 Simulation results

The state bounding observer has been applied to the state estimation of three systems. The first one is observable and detectable (O, D), the second one is non observable but detectable (NO, D) and the third one is neither observable nor detectable (NO, ND). The corresponding state space representations are given by (39) and Table 1.

$$A_k = \left[\begin{array}{ccc} a & & \\ \hline 1 & 0 & 0 \\ 0 & 1 & 0 \end{array}\right], \quad B_k = \begin{bmatrix} 1 \\ 0 \\ 0 \end{bmatrix}, \quad E_k = 0.01.I_{3\times3} \tag{39}$$

$$C_k = \left[\begin{array}{c} c \\ \hline I_{3\times3} \end{array}\right], \quad D_k = \left[\begin{array}{c} 0 \\ \hline 0_{3\times1} \end{array}\right], \quad F_k = \left[\begin{array}{c|c} 0.01 & 0_{1\times3} \\ \hline 0_{3\times1} & 10^6.I_{3\times3} \end{array}\right]$$

The last three lines of C_k, D_k and F_k are implemented in the observer algorithm in order to bound the state domain. They correspond to the above defined "artificial measurements" (3).

(A_k, c)	a	c
O, D	[2.548 –2.5165 0.94848]	[1 –2.7 1.4]
NO, D	[2.548 –2.5165 0.94848]	[1 –2.95 1.9]
NO, ND	[2.6 –2.5725 1.01475]	[1 –3.1 2.2]

Table 1: Parameters of the three systems under study

Figure 6 shows simulation results when d=5, u_k=0, $x_0=[4\ 4\ 4]^T$, $[\hat{x}_0]=[-5;5]^3$ (i.e. (2) holds) and v_k (resp. w_k) is a uniform random noise in $\square^n$ (resp. in $\square^p$).

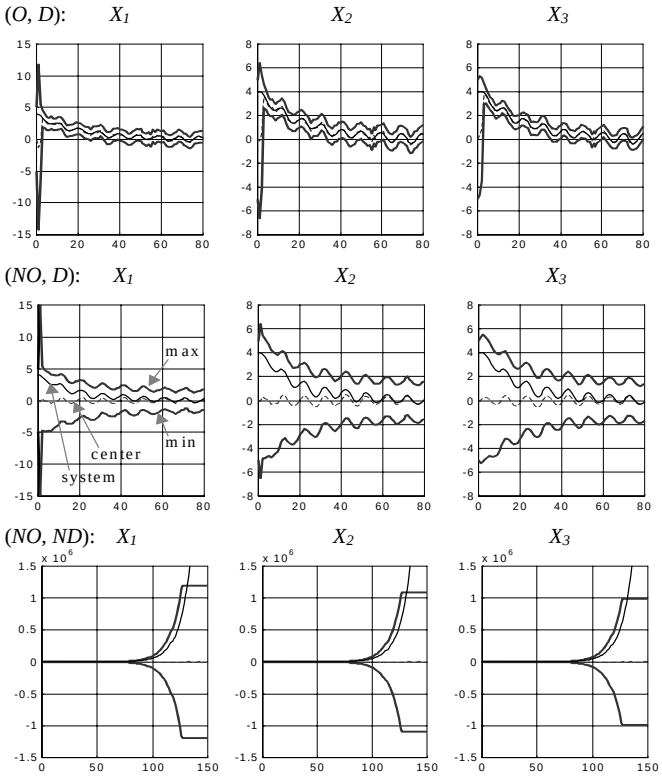

Figure 6: Responses of the state bounding observer

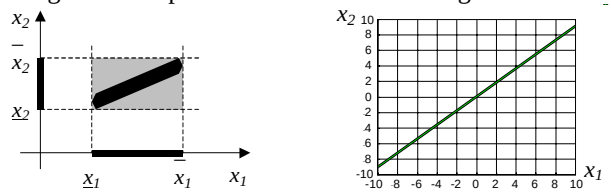

(a): State bounds at time k (b): (NO, ND), k=30, zoom

Figure 7: 1D and 2D projection of the estimated state domain

Each subplot in Figure 6 refers to the time responses related to one state (column-wise) and to one of the system under study (line-wise). Each subplot is composed of four curves: The min and max curves represent the state bounds computed from the interval hull of the zonotope describing the set of possible states at time k (Figure 7a). In Figure 6, the dotted lines correspond to the projection of the center of the estimated state domain. It is to be compared with the continuous line representing the time evolution of the system "real" state. Figure 6 shows the convergence of the state bounding observer, except for the (NO, ND) case. Convergence is fast in the (O, D) case and slower in the (NO, D) case. The (NO, D) system is composed of two observable oscillating poles and one unobservable real pole (z=0.95, $|z|<1$). The observer convergence, as shown by the state bounds, follows the dynamic involved by this later mode (Figure 6). The (NO, ND) case is also worth commenting. The "real" state remains inside the state bounds (until the "physical" bounds, 10^6, are reached (39), what occurs at k=125). Figure 6 could let believe that the state information is very inaccurate (i.e. the bounds related to the three states diverge). A 2D projection of the zonotope representing the set of possible states at k=30 (Figure 7b) shows that the increasing inaccuracy is oriented toward a single direction. This direction is that of the unobservable subspace, $D_{NO}=[0.631\ \ 0.574\ \ 0.522]^T$. Figure 7b allows to check that the principal direction of the state domain projection is parallel to $[0.631\ \ 0.574]^T$ (projection in the plane (x_1,x_2)).

5 Conclusion

The proposed state-bounding observer shows that zonotopes may be a suitable alternative to other domain representations. The resulting algorithm reduces to rather simple and fast matrix computations. Moreover, the wrapping effect that is often critical when integrating uncertain dynamical systems, can be controlled through the parameterization of domains complexity. Simulation results show the effectiveness of the proposed correction step. Quantifying the pessimism induced by the successive outer approximations could however be useful to study, optimize and compare several reduction and correction strategies. Comparisons on benchmarks with Kalman filters and other existing state bounding observers also seem necessary to assess more precisely the potential fields for the future applications of zonotope based observers.

References

[1] P. Bouron, D. Meizel, Ph. Bonnifait, "Set-membership non-linear observers with application to vehicule localisation", ECC'2001, Porto, Portugal (2001).

[2] C. Durieu, L. Loron, E. Sedda, I. Zein, "Fault detection of an induction motor by set-membership filtering and Kalman filtering", ECC'99, Karlsruhe, Germany (1999).

[3] C. Durieu, E. Walter, B. Polyak, "Multi-Input, multi-output ellipsoidal state bounding", Journal of optimization theory and applications, Vol. **111**, No. 2, pp. 273-303, (2001).

[4] L. Jaulin, M. Kieffer, O. Didrit, E. Walter, "Applied interval analysis", Springer-Verlag (2001).

[5] W. Kühn, "Rigorously computed orbits of dynamical systems without the wrapping effect", Computing, **61**, pp. 47-67, (1998).

[6] W. Kühn, "Towards an optimal control of the wrapping effect", SCAN'98, IMACS/GAMM International symposium on scientific computing, computer arithmetic and validated numerics, Budapest, Hungary (1998).

[7] W. Kühn, "Zonotope Dynamics in numerical quality control", in Mathematical Visualization, H.-C. Hege, K. Polthiers (eds.), pp 125-134, Springer (1998).

[8] S. Lesecq, A. Barraud, "Off-line diagnosis using output error membership set estimation : application to induction motor", Proceeding of IFAC Safeprocess'2000, Vol. **2**, pp. 1163-1167, Budapest, Hungary (2000).

[9] H. Sorenson (ed.), "Special issue on applications of Kalman filtering", IEEE Transactions on Automatic Control, Vol. **28**, No. 3, pp. 253-434, (1983).